



Universiteit  
Leiden  
The Netherlands

## Unravelling glycosylation reaction mechanisms

Vrande, K.N.A. van de

### Citation

Vrande, K. N. A. van de. (2025, October 9). *Unravelling glycosylation reaction mechanisms*. Retrieved from <https://hdl.handle.net/1887/4266985>

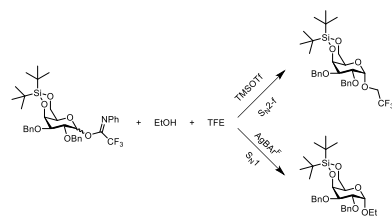
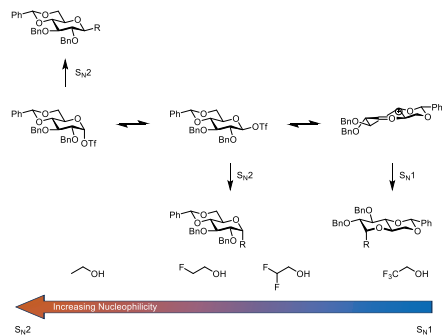
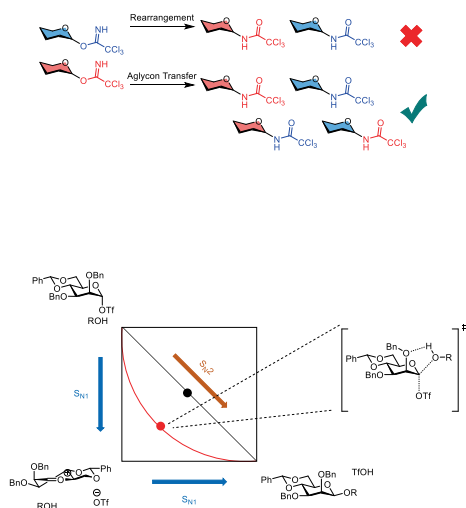
Version: Publisher's Version

License: [Licence agreement concerning inclusion of doctoral thesis in the Institutional Repository of the University of Leiden](#)

Downloaded from: <https://hdl.handle.net/1887/4266985>

**Note:** To cite this publication please use the final published version (if applicable).

## Chapter 6: Summary and Future Prospects

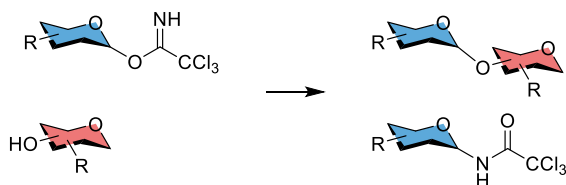


## Summary

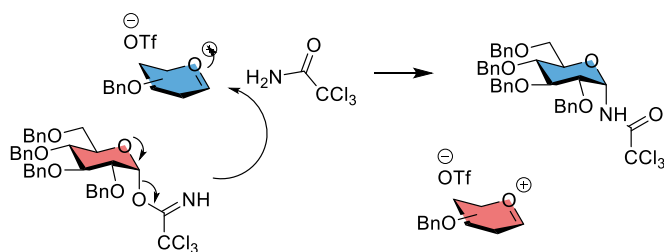
A key step in the synthesis of oligosaccharides and glycoconjugates is the formation of the glycosidic bond. The stereoselective formation of glycosidic bonds, however, can be difficult and whereas 1,2-*trans* bonds can easily be formed by the participation of the protective group on the C-2 position, no general methodology exists for the synthesis of 1,2-*cis* glycosidic bonds. Furthermore, the formation of these bonds does not take place via a clear-cut single-reaction mechanism. Instead, the mechanism that is followed lies somewhere on the spectrum between the  $S_N1$  and  $S_N2$  reaction mechanisms, involving different reactive intermediates, ranging from covalent ones to ion pairs. These, in combination with the reactivity of the incoming nucleophile, play a crucial role in shaping the outcome of a glycosylation reaction. The aim of this thesis is to study glycosylation reaction mechanisms in a systematic manner by making use of physical-chemical techniques that often rely on isotopic labelling.

In **Chapter 1**, an overview of various isotopic labelling techniques in carbohydrate chemistry is provided. These include both techniques to clarify the structure of a carbohydrate or products formed after a reaction of these carbohydrates as well as applications of isotope labelling to investigate reaction mechanisms, and they can entail the 'simple' labelling of a specific atom to see where it ends up after a reaction or sophisticated studies of intermediates by NMR spectroscopy and the establishment of Kinetic Isotope Effects (KIEs). **Chapter 2** describes a series of  $^{13}\text{C}$  and  $^{15}\text{N}$  cross-over experiments to investigate the mechanism behind the 'rearrangement' of glycosyl trichloroacetimidate donors to the corresponding trichloroacetamides (see Scheme 1). This reaction is often assumed to take place via a rearrangement, as depicted in Scheme 1A. To investigate the mechanism of formation of the anomeric acetamides, a series of cross-over experiments was performed, whereby half of the donor contained an anomeric  $^{13}\text{C}$  label and the other half a  $^{15}\text{N}$  label in the imidate leaving group. Using a combination of  $^1\text{H}$ ,  $^{13}\text{C}$  and  $^{15}\text{N}$  NMR spectroscopy, it was shown that the acetamide product is formed through an aglycon transfer mechanism as depicted in Scheme 1B. In this mechanism, the activated glycosyl donor is attacked by the imidate-NH of another donor molecule, activating the second donor molecule in the process.

A



B



**Scheme 1:** (A) The “rearrangement” of anomeric trichloroacetimidates to give the trichloroacetamides. (B) The reaction mechanism involves an aglycon transfer process, as confirmed by the experiments performed in Chapter 2.

The glycosylation reaction mechanism of benzylidene-protected glucose donor **1** (Figure 1) was investigated using KIEs in **Chapter 3**. Both primary  $^{13}\text{C}$  and secondary  $^2\text{H}$  KIEs were used. The series of acceptors **2-5** was chosen for their gradually decreasing nucleophilicity, while alcohol **6** was investigated to map the effect of the steric difference with **2**, and **7** was used as it is known to react in an  $\text{S}_{\text{N}}1$ -like fashion and therefore serves to benchmark the  $\text{S}_{\text{N}}1$  side of the KIE values. The results of the KIE experiments showed that the  $\beta$ -products were formed through an  $\text{S}_{\text{N}}2$ -like reaction mechanism. For the  $\alpha$ -products, a gradual shift from an  $\text{S}_{\text{N}}2$ -type to an  $\text{S}_{\text{N}}1$ -type mechanism was revealed when going down the series from the most nucleophilic alcohol **2** to the least nucleophilic one **5**. Acceptor **6** reacted with somewhat more  $\text{S}_{\text{N}}1$  character than **2**, and acceptor **7** reacted via an  $\text{S}_{\text{N}}1$  mechanism, as expected. These results provide detailed insight into how reaction mechanisms can change as a function of acceptor nucleophilicity and they establish a benchmark to study other glycosylation reactions.

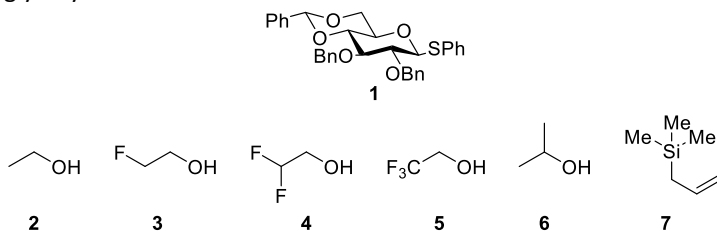


**Figure 1:** Donor (**1**) and acceptors (**2-7**) used to measure the KIEs.

Building on the results obtained in Chapter 3, **Chapter 4** used the same KIE techniques to investigate the mechanism of the  $\beta$ -Crich mannosylation reaction using donor **8** (Figure 2A). Again, the series of acceptors with decreasing nucleophilicity was chosen to systematically study the effect of the acceptor on the reaction mechanism. Contrary to the results found for glucose donor **1**, the KIEs did not vary significantly upon changing the acceptor. The obtained KIE values were all rather similar and fell between the values associated with  $S_N1$  or  $S_N2$  reactions. From these results, it was concluded that the glycosylation reactions with donor **8** take place via an ‘exploded’ transition state: an  $S_N2$ -like transition state, but with significant  $S_N1$  character due to the large carbon-nucleophile and carbon-leaving group distances. A possible explanation for the lack of development of the reaction mechanism relative to acceptor nucleophilicity is given in the transition state in Figure 2B. The hydrogen bond between the incoming nucleophile and the protected alcohol at the C-2 position increases in strength with decreasing acceptor nucleophilicity and compensates for the loss of acceptor reactivity when going from stronger to weaker nucleophiles.

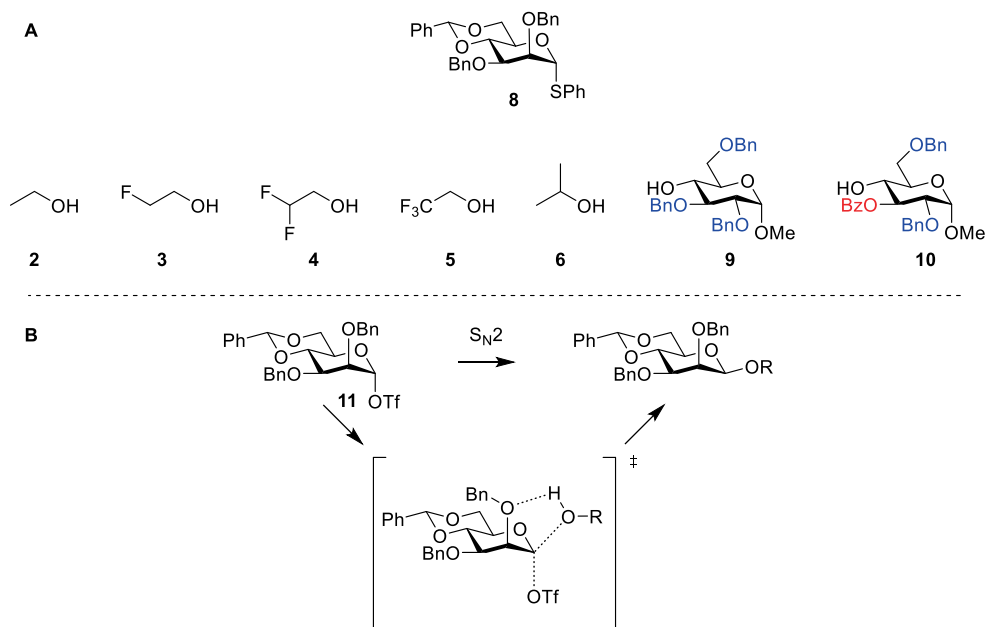


**Figure 2:** (A) Donor (**8**) and acceptors (**2-6**, **9**, **10**) used to study the KIEs. (B) Exploded transition state with possible hydrogen bond formation.

In the final chapter, **Chapter 5**, competition experiments between two acceptors were performed to investigate the relative reactivity of the acceptors. To this end, both the  $\beta$ -selective galactose donor **12** and  $\alpha$ -selective donor **13** were used (Figure 3). Since **12** is generally considered to react in an  $S_N2$  mechanism and **13** via an  $S_N1$  mechanism, this allowed investigation of the influence of the mechanism on the relative acceptor reactivity. The results for donor **12** were in line with previously established relationships between acceptor structure and reactivity, where the donor reacted faster with the more electron-

rich acceptor. Donor **13**, on the other hand, reacted faster with the least electron-rich acceptor when activated with TMSOTf. To better understand these unexpected results, competition experiments were conducted, in which **13** was activated using a combination of TMSI and AgBAR<sup>F</sup>. Under these conditions, the most electron-rich acceptor was the fastest reaction partner. Since the BAR<sup>F(-)</sup> anion is known to be a non-coordinating anion, it was assumed that activation of **13** with TMSI-AgBAR<sup>F</sup> leads to a pure S<sub>N</sub>1 mechanism. To account for the relative reactivity of the acceptors in the experiments in which **13** was activated with TMSOTf, the front-face S<sub>N</sub>2-f reaction mechanism depicted in Scheme 3 was forwarded. The hydrogen bond in transition state **14** explains why electron-poor acceptors are more reactive under these conditions: electron-poor acceptors are generally more acidic, strengthening the hydrogen bond and, thus the transition state, compared to more electron-rich acceptors.

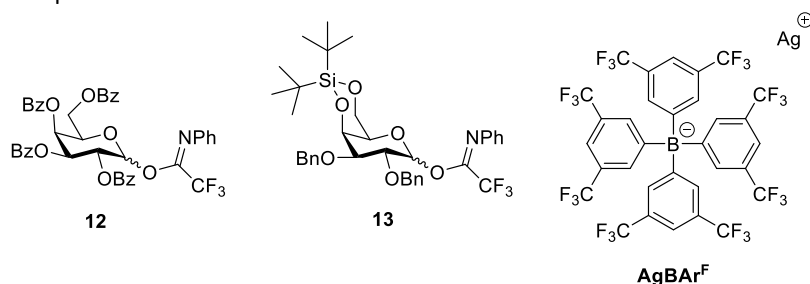
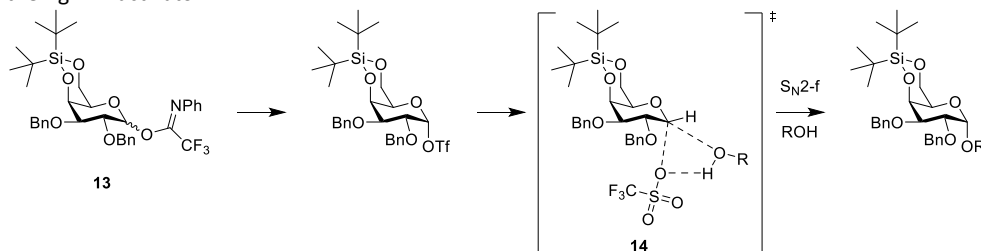


**Figure 3:** Structures of donors used for the competition experiments in Chapter 5 and the structure of the AgBAR<sup>F</sup> activator.



**Scheme 3:** Transition state of the front-face S<sub>N</sub>2 reaction.

## Future Prospects

### KIEs of Glucosazide Donors

When comparing glycosylation reactions of benzylidene glucose donor **1** to those of its glucosazide counterpart **15** (Figure 4), it can be seen that donor **15** is more  $\beta$ -selective than **1**, although the trend that more  $\alpha$ -product is formed from acceptors of decreasing nucleophilicity is maintained.<sup>1-3</sup> It may be speculated that the increase in  $\beta$ -selectivity originates from the enhanced stability of the anomeric triflates, and the decreased stability of the intermediate glucosazide oxocarbenium ion, shifting the substitution mechanisms to the S<sub>N</sub>2-side of the reaction pathway continuum. In this thesis, it was shown that the  $\beta$ -products formed from glucose donor **1**, were the result of an S<sub>N</sub>2-like attack on the  $\alpha$ -triflates, and this pathway was preferred by strong nucleophiles. In the case of mannose

donor **8** (Figure 2), the  $\beta$ -selectivity resulted from an exploded transition state. To examine the transition states on the reaction pathways of donor **15**, a series of systematic KIE experiments similar to those described in chapters 3 and 4 can be performed using donor **15**. This would answer the question where the enhanced  $\beta$ -selectivity of donor **15** originates from, and expand the understanding of the effect of functional groups on the glycosylation reaction mechanism.

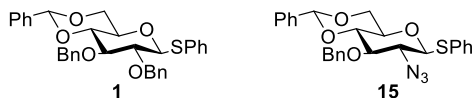


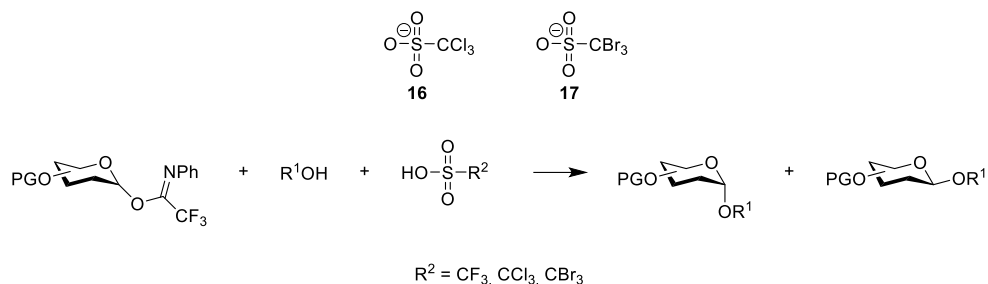
**Figure 4:** Structure of benzylidene protected glucose (**1**) and glucosazide (**15**) donors.

### Measuring the KIEs of AgBAR<sup>F</sup> Activated Reactions

In Chapter 5, glycosylation reactions were performed with a silylene-protected galactosyl donor using TMSI-AgBAR<sup>F</sup> as an activator instead of the commonly used triflate-based activators. Since the BAR<sup>F</sup> anion is known to be a non-coordinating anion, these reactions are expected to follow an S<sub>N</sub>1 pathway.<sup>4-6</sup> To further examine the reaction mechanism, KIE experiments can be performed on glycosyl donors activated with AgBAR<sup>F</sup>. To this end, a systematic method similar to the one described in chapters 3 and 4 is proposed, where a series of acceptors with decreasing nucleophilicity (EtOH-TFE) will be used, in addition to interesting examples of carbohydrate and carbon nucleophile acceptors. Additionally, NMR spectroscopy can be used to characterise the intermediates that are involved in this reaction. Preliminary results have shown that upon the addition of TMSI to the reaction mixture, the anomeric iodide is formed, and this intermediate disappears upon the addition of AgBAR<sup>F</sup>.

### Systematic Study of Leaving Group Effects

In Chapter 5, it was found that, next to the nature of the donor and acceptor, the type of leaving group critically influences the glycosylation reaction. To study the effect of the leaving group capacity in a systematic manner, the two 'larger siblings' of the commonly used triflate leaving group, namely the trichlate (**16**)<sup>7</sup> and tribrate (**17**)<sup>8</sup> anions, depicted in Scheme 4, are of interest and these have been synthesised and characterised by Mertens *et al.*. The effect of these leaving groups could be investigated using the model reaction depicted in Scheme 4, where an imidate glycosyl donor is activated with the conjugate acid of the triflate, trichlate and tribrates. Using the benzylidene glucoside donor, both the reaction yield and  $\alpha:\beta$  ratio can be measured to link these to the reactivity and mechanism of the reaction. Also, the use of the silylene galactose system is of interest as work in this thesis has indicated that the formation of an H-bond between the leaving group and the incoming acceptor is a decisive factor.



**Scheme 4:** Structure of trichlate (**16**) and tribrate (**17**) anions and proposed reaction scheme to investigate leaving group effects.

### Bistriflimide

The  $\text{BAR}^{\text{F}}$  anion used in Chapter 5 is not the only known non-coordinating anion. Another example, which has seen use in glycosylation reactions before, is the bistriflimide (**18**,  $\text{Tf}_2\text{N}^-$ ) anion, depicted in Figure 4.<sup>9</sup> The silver salt of this anion,  $\text{AgNTf}_2$ , is known as an additive in the gold-catalysed glycosylation reactions<sup>10,11</sup> and it has also been used as an activator for glycosyl ynone donors.<sup>12</sup> Furthermore, it has been shown that the use of  $\text{TMSNTf}_2$  or  $\text{HNTf}_2$  as the catalyst to activate trichloroacetimidate glycosylation donors can provide highly stereoselective glycosylation reactions that seem to proceed with inversion of the stereochemistry of the starting donor.<sup>13</sup> The bistriflimide leaving group would be an interesting intermediate between the triflate and  $\text{BAR}^{\text{F}}$  leaving groups: it does not coordinate as strongly as the triflate and it should give more  $\text{S}_{\text{N}}1$ -like reactions but should be able to form hydrogen bonds through the triflimide nitrogen or oxygen atoms. The competition experiments as described in Chapter 5 will shed light on the effect of this leaving group. These results can then be expanded upon by performing KIE experiments, to see if a more  $\text{S}_{\text{N}}1$ -like or more  $\text{S}_{\text{N}}2$ -like reaction takes place.

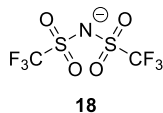


**Figure 5:** Structure of the bistriflimide ( $\text{Tf}_2\text{N}^-$ ) anion.



## References and Notes

1. van der Vorm, S.; van Hengst, J. M. A.; Bakker, M.; Overkleeft, H. S.; van der Marel, G. A.; Codée, J. D. C. Mapping the Relationship between Glycosyl Acceptor Reactivity and Glycosylation Stereoselectivity. *Angew Chem* **2018**, *130* (27), 8372–8376. <https://doi.org/10.1002/ange.201802899>.
2. van Hengst, J. M. A.; Hellemans, R. J. C.; Remmerswaal, W. A.; van de Vrande, K. N. A.; Hansen, T.; van der Vorm, S.; Overkleeft, H. S.; van der Marel, G. A.; Codée, J. D. C. Mapping the Effect of Configuration and Protecting Group Pattern on Glycosyl Acceptor Reactivity. *Chem Sci* **2023**, *14* (6), 1532–1542. <https://doi.org/10.1039/d2sc06139b>.
3. Van der Vorm, S.; Overkleeft, H. S.; Van der Marel, G. A.; Codée, J. D. C. Stereoselectivity of Conformationally Restricted Glucosazide Donors. *J Org Chem* **2017**, *82* (9), 4793–4811. <https://doi.org/10.1021/acs.joc.7b00470>.
4. Nishida, H.; Takada, N.; Yoshimura, M.; Sonoda, T.; Kobayashi, H. Tetrakis[3,5bis(Trifluoromethyl)Phenyl]Borate. Highly Lipophilic Stable Anionic Agent for Solvent-Extraction of Cations. *Bull Chem Soc Jpn* **1984**, *57* (9), 2600–2604. <https://doi.org/https://doi.org/10.1246/bcsj.57.2600>.
5. Krossing, I.; Raabe, I. Noncoordinating Anions - Fact or Fiction? A Survey of Likely Candidates. *Angew Chem Int Ed* **2004**, *43* (16), 2066–2090. <https://doi.org/10.1002/anie.200300620>.
6. Brookhart, M.; Grant, B.; Volpe, A. F. [(3,5-(CF<sub>3</sub>)<sub>2</sub>C<sub>6</sub>H<sub>3</sub>)<sub>4</sub>B]-[H(OEt)<sub>2</sub>]<sup>+</sup>: A Convenient Reagent for Generation and Stabilization of Cationic, Highly Electrophilic Organometallic Complexes. *Organometallics* **1992**, *11* (11), 3920–3922. <https://doi.org/https://doi.org/10.1021/om00059a071>.
7. Mertens, A.; van Gerven, D.; Kunert, I.; Wickleder, M. S. Trichlates, an Unattended Class of Compounds: Characterization of Cl<sub>3</sub>CSO<sub>2</sub>Cl, and (H<sub>5</sub>O<sub>2</sub>)[Cl<sub>3</sub>CSO<sub>3</sub>]. *Chem Eur J* **2023**, *29* (63). <https://doi.org/10.1002/chem.202302128>.
8. Mertens, A.; Eppers, K.; van Gerven, D.; Wickleder, M. S. Triflate's Bigger Brother: The Unprecedented Triborate Anion, [Br<sub>3</sub>CSO<sub>3</sub>]<sup>-</sup>. *Chem Eur J* **2024**, *30* (11). <https://doi.org/10.1002/chem.202303617>.
9. Zhao, W.; Sun, J. Triflimide (HNTf<sub>2</sub>) in Organic Synthesis. *Chem Rev* **2018**, *118* (20), 10349–10392. <https://doi.org/10.1021/acs.chemrev.8b00279>.
10. Zu, Y.; Cai, C.; Sheng, J.; Cheng, L.; Feng, Y.; Zhang, S.; Zhang, Q.; Chai, Y. N-Pentenyl-Type Glycosides for Catalytic Glycosylation and Their Application in Single-Catalyst One-Pot Oligosaccharide Assemblies. *Org Lett* **2019**, *21* (20), 8270–8274. <https://doi.org/10.1021/acs.orglett.9b03038>.
11. Wander, D. P. A.; Van Der Zanden, S. Y.; Vriends, M. B. L.; Van Veen, B. C.; Vlaming, J. G. C.; Bruyning, T.; Hansen, T.; Van Der Marel, G. A.; Overkleeft, H. S.; Neefjes, J. J. C.; Codée, J. D. C. Synthetic (N, N-Dimethyl)Doxorubicin Glycosyl Diastereomers to Dissect Modes of Action of Anthracycline Anticancer Drugs. *J Org Chem* **2021**, *86* (8), 5757–5770. <https://doi.org/10.1021/acs.joc.1c00220>.
12. Dong, X.; Chen, L.; Zheng, Z.; Ma, X.; Luo, Z.; Zhang, L. Silver-Catalyzed Stereoselective Formation of Glycosides Using Glycosyl Ynenoates as Donors. *Chem Comm* **2018**, *54* (62), 8626–8629. <https://doi.org/10.1039/c8cc02494d>.
13. Kowalska, K.; Pedersen, C. M. Catalytic Stereospecific O-Glycosylation. *Chem Comm* **2017**, *53* (12), 2040–2043. <https://doi.org/10.1039/c6cc10076g>.